Nonlinear response for nonautonomous systems

Janka Petravic and Denis J. Evans
Research School of Chemistry, Australian National University, Canberra, Australian Capital Territory 0200, Australia
(Received 18 February 1997)

We present a detailed derivation of the transient time correlation function (TTCF) form of nonlinear response theory which is generalized to handle time-dependent external fields. Our derivation stresses the analogy with the TTCF formalism for constant fields. We also discuss some limiting cases. We use computer simulation to test the generalized TTCF theory. Our simulation results show that the generalized TTCF method has an efficiency superior to direct calculation not only for weak fields but also for strong time-dependent external fields. [S1063-651X(97)10607-9]

PACS number(s): 02.70.Ns, 05.20.−y, 61.20.Ja, 61.20.Lc

I. INTRODUCTION

For classical N-body systems close to equilibrium, the Green-Kubo linear response theory [1,2] provides a relatively complete treatment of response to both constant and time-dependent external fields. Far from equilibrium a statistical mechanical description of nonequilibrium steady states in constant external fields is given by the transient time correlation function (TTCF) [3] and Kawasaki [4] formalisms. The transient time correlation function is a nonlinear analog of the Green-Kubo equilibrium time correlation function. The TTCF method is perhaps the simplest nonlinear generalization of the Green-Kubo relations. It is valid for both thermostated and unthermostated nonlinear dissipative systems.

In a previous letter [5], we outlined how this method can be generalized to describe the nonlinear response to time-dependent external fields, using the concept of an extended phase space where an additional coordinate characterizes the time dependence of the external field. Previous theories [6] relied upon the definition of propagators using time-ordered exponentials, and the resulting expressions, due to commutivity constraints, were too complex to be used in comparisons with experiment. Our theory gives an expression for the response which is analogous to the simple TTCF expression for a constant field, and the algorithm using this expression exhibits an efficiency which is superior to direct simulation both for weak and strong applied fields.

In Sec. II of this paper we derive the generalized time-dependent response of a phase function (i.e., a function of the phase-space coordinates), emphasizing the analogy with the TTCF response theory for a constant field, and discuss the limiting cases of constant field TTCF and linear time-dependent response. We test the formalism using computer simulation of a two-disk color conductivity model described in Sec. III. In Secs. IV and V, we compare the results and efficiency of direct calculation, Green-Kubo theory, and time-dependent TTCF theory for the response of a phase function with a strong linear component and with no linear component, respectively.

II. FORMALISM

First we outline the TTCF response theory for N-particle systems in a constant external field F_e switched on at $t=0$. The equations of motion of such a system are

$$\dot{\mathbf{q}}_i=\frac{\mathbf{p}_i}{m}+\mathbf{C}_i(\mathbf{\Gamma})F_e\,,$$

$$\dot{\mathbf{p}}_i=\mathbf{F}_i+\mathbf{D}_i(\mathbf{\Gamma})F_e-\alpha\mathbf{p}_i\,, \tag{1}$$

where $\mathbf{F}_i$ is the interaction force between the particles, and the Gaussian thermostat multiplier α, given by

$$\alpha=\frac{\sum_i \frac{\mathbf{F}_i}{m}\cdot\mathbf{p}_i}{\sum_i \frac{\mathbf{p}_i^2}{m}}+\frac{\sum_i \frac{\mathbf{D}_i}{m}\cdot\mathbf{p}_i}{\sum_i \frac{\mathbf{p}_i^2}{m}}F_e\,, \tag{2}$$

makes the kinetic energy $K=\Sigma_i\mathbf{p}_i^2/2m$ a constant of motion. The state of the system can be represented by a point in the phase space $\mathbf{\Gamma}$ spanned by $(\mathbf{q}_i,\mathbf{p}_i\ (i=1,\ldots,N))$.

Let $B(\mathbf{\Gamma})$ be a phase function, i.e., a function of the phase-space coordinates $\mathbf{q}_i$ and $\mathbf{p}_i$ only. For $t\leqslant 0$, the external field is zero, the system is assumed to be at equilibrium and the phase space average $\langle B(t<0)\rangle$ is equal to its equilibrium value $\langle B(0)\rangle$. For $t>0$, the constant field acts upon the system, and the phase-space average of B changes

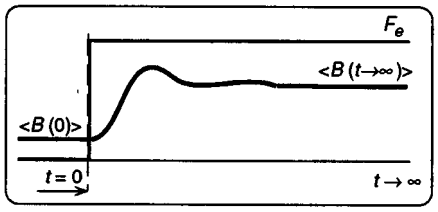

FIG. 1. Response of a phase function B to a constant field F_e applied at $t=0$. The phase space average $\langle B\rangle$ changes from its equilibrium value $\langle B(0)\rangle$, through transient behavior toward a constant steady-state value $\langle B(t\to\infty)\rangle$.

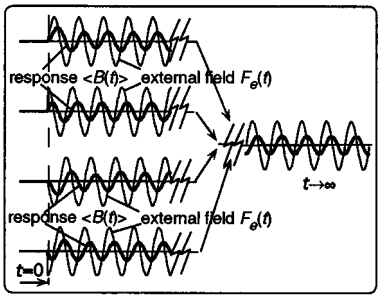

FIG. 2. Response of a phase function B to a time-periodic external field F_e applied at $t=0$. At first the response depends strongly on the initial ''phase angle'' of the external field. After a long time, the time dependence of the responses to fields with different initial ''phase angles'' will be different, but their dependence on the ''phase angle'' will be the same.

through transients to its steady-state value $\langle B(t\to\infty)\rangle$, as shown in Fig. 1. The TTCF theory relates the instantaneous value of the phase-space average $\langle B(t)\rangle$ to the time integral of the field-dependent correlation function of $B(\mathbf{\Gamma})$ and the dissipative flux $J(\mathbf{\Gamma})$,

$$\langle B(t)\rangle=\langle B(0)\rangle-\beta F_e\int_0^t ds\langle B[\mathbf{\Gamma}(s)]J[\mathbf{\Gamma}(0)]\rangle. \quad (3)$$

In Eq. (3), $\beta=1/k_BT$, where k_B is the Boltzmann constant, T is the absolute temperature, and the dissipative flux $J(\mathbf{\Gamma})$ is defined as

$$J(\mathbf{\Gamma})=\sum_i\left(\mathbf{C}_i\cdot\mathbf{F}_i-\mathbf{D}_i\cdot\frac{\mathbf{p}_i}{m}\right). \quad (4)$$

Expression (3) has been derived using the assumption of adiabatic incompressibility of phase space ($AI\mathbf{\Gamma}$), namely,

$$\sum_i\left(\frac{\partial}{\partial\mathbf{q}_i}\cdot\mathbf{C}_i+\frac{\partial}{\partial\mathbf{p}_i}\cdot\mathbf{D}_i\right)=0, \quad (5)$$

which is satisfied by all systems whose adiabatic equations of motion can be derived from a Hamiltonian—see Ref. [7] for details. The time dependence on both sides is generated from the field-dependent equations of motion for system (1), with or without the thermostat. The validity of the Eq. (3) also relies upon the fact that Eqs. (1) do not depend explicitly on time, and therefore Eq. (3) does not hold in the nonautonomous case.

If the external field is periodic in time with the period T_e, $F_e=F_e(t)=F_e(t+T_e)$, there is no real steady state. In the long-time limit the response of a phase function will be time periodic. However, regardless of where, within its period, the field is switched on at $t=0$, in the long-time limit the response $\langle B(t\to\infty)\rangle$ will depend *on the external field* (not time) in the same way, as shown in Fig. 2. This means that after a long time the response will have the same value at the same point in the period of $F_e(t)$ irrespective of the starting ''phase angle'' of $F_e(t)$ at $t=0$. Clearly this lack of sensitivity to the initial phase angle will eventually break down if the external field is sufficiently strong. We do not consider such systems here.

Therefore it is convenient to define an additional phase coordinate φ proportional to time and analogous to the phase angle of trigonometric functions,

$$\varphi(t)=\varphi+\omega t,$$

so that F_e becomes a periodic function of φ, $F_e(\varphi)=F_e(\varphi+\Phi_e)$, where $\Phi_e=\omega T_e$. The phase space of the system can be *extended* by adding this new coordinate, so that all the explicit time dependence in the equations of motion is contained in the variable φ,

$$\dot{\mathbf{q}}_i=\frac{\mathbf{p}_i}{m}+\mathbf{C}_i(\mathbf{\Gamma})F_e(\varphi),$$

$$\dot{\mathbf{p}}_i=\mathbf{F}_i+\mathbf{D}_i(\mathbf{\Gamma})F_e(\varphi)-\alpha\mathbf{p}_i \quad (6)$$

$$\dot{\varphi}=\omega.$$

The state of the system can now be represented by a point in *extended* phase space $\mathbf{\Gamma}'=(\mathbf{\Gamma},\varphi)=(\mathbf{q}_i,\mathbf{p}_i,\varphi;i=1,\ldots,N)$. It is sufficient to consider values of φ in the range $\varphi\in[0,\Phi_e]$, so that $\varphi(t)=\mathrm{mod}(\varphi+\omega t,\Phi_e)$. In order to know the response $\langle B(t)\rangle$ at a certain specified time t, we need to know the initial ''phase angle'' φ of the external field. At very long times $\langle B(t)\rangle$ is dependent on both the time t and the initial value of φ. For example, for any time t, no matter how large, the value of $\langle B(t)\rangle$ is different for different initial phase angles. Therefore we should write $\langle B(\varphi_0;t)\rangle$. However, at large times (provided the field strength is not too large) the value of $\langle B(t)\rangle$ is a unique function of the current value of φ, namely $\varphi(t)$, as illustrated in Fig. 2. There is no ambiguity in writing $\langle B(\varphi(t))\rangle$ in the long-time limit. The final state, which is time periodic in the phase space $\mathbf{\Gamma}$, is a time-*independent* steady state in the extended phase space $\mathbf{\Gamma}'$.

Since system (1) in a time-dependent external field $F_e(t)$ is now described by autonomous equations of motion (6) in the extended phase space, we can repeat the steps in the derivation of TTCF response for autonomous systems (3) and evaluate the *extended phase-space average* $\langle B(t)\rangle'$ of $B(\mathbf{\Gamma})$ at time t. We shall go through these steps explicitly below.

Although $B(\mathbf{\Gamma})$ is solely a function of $\mathbf{\Gamma}$, the phase $\mathbf{\Gamma}$ that the system evolves to at time t, namely, $\mathbf{\Gamma}(t)$, is a function of the initial *extended* phase, $\mathbf{\Gamma}'=(\mathbf{\Gamma},\varphi)$. Thus it is more revealing to write $B(\mathbf{\Gamma}(t))=B(\mathbf{\Gamma}(t;\mathbf{\Gamma},\varphi))$. In order to know the value of a phase function at time t, in addition to the elapsed time, we need to specify the initial phase vector $\mathbf{\Gamma}$ and the initial phase angle φ of the external field.

For systems governed by Eq. (6), the equilibrium extended phase-space distribution $f_0'(\mathbf{\Gamma}')$ is uniform in φ,

$$f_0'(\mathbf{\Gamma}')d\mathbf{\Gamma}'=\frac{f_0(\mathbf{\Gamma})}{\omega T_e}\,d\mathbf{\Gamma}\,d\varphi, \quad (7)$$

where

$$f_0(\mathbf{\Gamma})=\frac{\exp[-\beta U(\mathbf{\Gamma})]\,\delta(K(\mathbf{\Gamma})-K_0)}{\int d\mathbf{\Gamma}\,\exp[-\beta U(\mathbf{\Gamma})]\,\delta(K(\mathbf{\Gamma})-K_0)}.$$

Here U is the potential energy of the system, $K_0 = dN/2\beta$ is the conserved kinetic energy, and d is the Cartesian dimensionality of the system.

The average over the extended phase space of B, taken at time t, is

$$\begin{aligned}\langle B(t)\rangle' &= \int d\mathbf{\Gamma}' f'(\mathbf{\Gamma}',t) B(\mathbf{\Gamma}) \\ &= \int d\mathbf{\Gamma}' f'(\mathbf{\Gamma}',0) B(\mathbf{\Gamma}(t;\mathbf{\Gamma}')) \\ &= \int d\mathbf{\Gamma}' f_0'(\mathbf{\Gamma}') B(\mathbf{\Gamma}(t;\mathbf{\Gamma},\varphi)) \\ &= \int d\mathbf{\Gamma} d\varphi \, \frac{f_0(\mathbf{\Gamma})}{\omega T_e} \, B(\mathbf{\Gamma}(t;\mathbf{\Gamma},\varphi)) \end{aligned} \tag{8}$$

in the Schrödinger and Heisenberg pictures, respectively. As the equilibrium distribution $f_0(\mathbf{\Gamma}')$ is known and given by Eq. (7), it is simpler to use the Heisenberg picture.

The equation of motion for $B(\mathbf{\Gamma})$ can be written using the chain rule

$$\frac{dB(\mathbf{\Gamma}(t))}{dt} = \dot{\Gamma} \cdot \frac{\partial}{\partial \mathbf{\Gamma}} [B(\mathbf{\Gamma})] \Big|_{\mathbf{\Gamma}(t)=\mathbf{\Gamma}(t;\mathbf{\Gamma},\varphi)} . \tag{9}$$

Differentiation of the Heisenberg expression (8) for $\langle B(t)\rangle$ using Eq. (9), and the fact that $\partial B/\partial\varphi = 0$, yields

$$\frac{d\langle B(t)\rangle'}{dt} = \int d\mathbf{\Gamma}' f_0'(\mathbf{\Gamma}') \left[\dot{\mathbf{\Gamma}}' \cdot \frac{\partial}{\partial \mathbf{\Gamma}'} (B(\mathbf{\Gamma})) \right]_{\mathbf{\Gamma}'(t)} . \tag{10}$$

Equality (10) relies upon the time independence of system (6), and does not hold in the non-autonomous case. Integrating Eq. (10) by parts, we obtain

$$\frac{d\langle B(t)\rangle'}{dt} = -\int d\mathbf{\Gamma}' B(\mathbf{\Gamma}(t)) \left[\frac{\partial}{\partial \mathbf{\Gamma}'} \cdot (\dot{\mathbf{\Gamma}}' f_0'(\mathbf{\Gamma}')) \right], \tag{11}$$

since the boundary term vanishes. Using the equations of motion (6), expression (7) for the equilibrium distribution function $f_0'(\mathbf{\Gamma}')$ and the definition of the dissipative flux (4), and assuming the adiabatic incompressibility of the phase space $AI\mathbf{\Gamma}$, Eq. (5), we get

$$\begin{aligned}\frac{\partial}{\partial \mathbf{\Gamma}'} \cdot [\dot{\mathbf{\Gamma}}' f_0'(\mathbf{\Gamma}')] &= \frac{\partial}{\partial \mathbf{\Gamma}} \cdot [\dot{\mathbf{\Gamma}} f_0'(\mathbf{\Gamma}')] \Big|_{t=0} + \omega \, \frac{\partial f_0'(\mathbf{\Gamma}')}{\partial \varphi} \Big|_{t=0} \\ &= f_0'(\mathbf{\Gamma}') \{\beta F_e(\varphi) J(\mathbf{\Gamma})\}_{t=0} . \end{aligned} \tag{12}$$

Substituting Eq. (12) into the equation of motion for Eq. (11), gives

$$\frac{d\langle B(t)\rangle'}{dt} = -\beta \int d\mathbf{\Gamma}' B(\mathbf{\Gamma}(t;\mathbf{\Gamma},\varphi)) F_e(\varphi) J(\mathbf{\Gamma}) f_0'(\mathbf{\Gamma}'),$$

and, integrating with respect to time yields

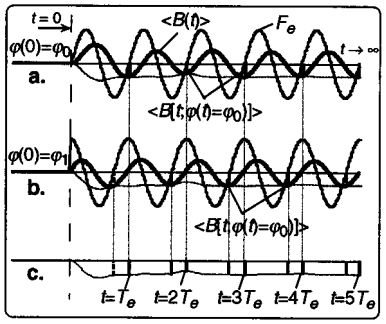

FIG. 3. A method to obtain a continuous response to a time-periodic field at a fixed value of ''phase angle'' φ. It is necessary to use the data from the responses starting at all possible initial $\varphi(0)$.

$$\begin{aligned}\langle B(t)\rangle' = \langle B(0)\rangle' - \beta \int_0^t ds \langle B[\mathbf{\Gamma}(s;\mathbf{\Gamma}(0),\varphi(0))] \\ \times F_e(\varphi(0)) J(\mathbf{\Gamma}(0))\rangle' . \end{aligned} \tag{13}$$

Expression (13) describes the evolution of the extended phase-space average of the phase variable after the external field is applied. The average over the *extended* phase space means an average over all possible initial combinations of positions, momenta and the additional phase-space coordinate φ. If B were taken to be the dissipative flux, then $\langle J(t)\rangle' = 0$, by symmetry. The fact that the extended average of the dissipative flux vanishes illustrates that the average taken in Eq. (13) is not really what we are most interested in. We shall now consider averages taken over the standard phase space $\mathbf{\Gamma}$ for a particular value of $\varphi = \varphi_P$ at time t.

As shown in Fig. 2, the long-time behavior of a phase function $\langle B(t)\rangle$ can be regarded as $\langle B(t)\rangle$ having a different ''steady state'' for each $\varphi(t) \in [0,\Phi_e]$. Let us investigate this idea in more detail. If the field is switched on at $t=0$ in such a way that $\varphi(t=0)=\varphi_0$, the response $\langle B(t)\rangle$ may look like the curve in Fig. 3(a). Since $\varphi(t) = \mathrm{mod}(\varphi+\omega t, \omega T_e)$, the value of $\varphi=\varphi_0$ occurs after each period T_e. We can monitor the corresponding value of the response $\langle B(t;\varphi(t)=\varphi_0)\rangle$ whenever the ''phase angle'' takes on the value of φ_0. It changes from the equilibrium value $\langle B(0)\rangle$ for $\varphi(t=0)=\varphi_0$ through several different values $\langle B(T_e;\varphi(T_e)=\varphi_0)\rangle$, $\langle B(2T_e;\varphi(2T_e)=\varphi_0)\rangle$,..., over a few periods, and after a long time it reaches its ''steady state'' and stays constant. However, the evolution of the responses for each φ_0 toward its ''steady state'' is not continuous in time as for the constant field, but we can only obtain discrete values one period T_e apart in time.

For φ_0 to occur at a time different from $t=0,T_e,2T_e,3T_e,\ldots$, the external field has to start differently at $t=0$, for example, like in Fig. 3(b), with $\varphi(t=0)=\varphi_1$. In this case, $\varphi(t)=\varphi_0$ occurs at $t=t_1, t_1+T_e, t_1+2T_e, t_1+3T_e \ldots$. If we included all possible starting points of the field $\varphi(t=0)\in[0,\Phi_e]$, we would obtain a continuous response $\langle B(t;\varphi(t)=\varphi_0)\rangle$ as a function of time for any ''phase angle'' φ_0, as shown by the dotted line in Fig. 3(c). However, each value of this continuous function within one period is a contribution of a different ensemble of systems, corresponding to the external field starting with a different ''phase angle'' at $t=0$. In other words, we have to use the

phase-space trajectories from the whole *extended* phase space $\mathbf{\Gamma}'$ in order to obtain a continuous time evolution of the response for a chosen value of φ_0.

Since the correlation function

$$\langle B[\mathbf{\Gamma}(t;\mathbf{\Gamma}(0),\varphi(0))]F_e(\varphi(0))J(\mathbf{\Gamma}(0))\rangle$$

in Eq. (13) is an average of a phase function, we shall need this concept of a continuous evolution of a phase function for a particular value of $\varphi=\varphi_P$ in the derivation of averages taken over the standard phase space $\mathbf{\Gamma}$ for a particular value of $\varphi=\varphi_P$ at time t.

The expression corresponding to the Heisenberg picture in Eq. (8) is

$$\begin{aligned}\langle B(\mathbf{\Gamma}(t);\varphi(t))=\varphi_P\rangle &= \langle B[\mathbf{\Gamma}(t)\,\delta(\varphi(t)-\varphi_P)]\rangle' \\ &= \int d\mathbf{\Gamma}'\, f_0'(\mathbf{\Gamma}')B(\mathbf{\Gamma}(t;\mathbf{\Gamma},\varphi=\varphi_P-\omega t))\delta(\varphi(t)-\varphi_P).\end{aligned}$$

Differentiating with respect to time, we find using the same procedure as above,

$$\begin{aligned}\frac{d}{dt}\langle B[\mathbf{\Gamma}(t)]\delta(\varphi(t)-\varphi_P)\rangle' &= \int d\mathbf{\Gamma}'\, f_0'(\mathbf{\Gamma}')\dot{\mathbf{\Gamma}}'\cdot\frac{\partial}{\partial\mathbf{\Gamma}'}\left[B(\mathbf{\Gamma}(t;\mathbf{\Gamma},\varphi=\varphi_P-\omega t))\delta(\varphi(t)-\varphi_P)\right] \\ &= -\int d\mathbf{\Gamma}'\, B(\mathbf{\Gamma}(t;\mathbf{\Gamma},\varphi=\varphi_P-\omega t))\delta(\varphi(t)-\varphi_P)\frac{\partial}{\partial\mathbf{\Gamma}'}\cdot[\dot{\mathbf{\Gamma}}' f_0'(\mathbf{\Gamma}')] \\ &= -\beta\int d\mathbf{\Gamma}'\, B(\mathbf{\Gamma}(t;\mathbf{\Gamma},\varphi=\varphi_P-\omega t))\delta(\varphi(t)-\varphi_P)F_e(\varphi)J(\mathbf{\Gamma})f_0'(\mathbf{\Gamma}') \\ &= -\beta\langle B(\mathbf{\Gamma}(t);\varphi(t)=\varphi_P)F_e(\varphi_P-\omega t)J(\mathbf{\Gamma}(0),\varphi_P-\omega t)\rangle \qquad (14)\end{aligned}$$

Integrating this equation gives

$$\begin{aligned}\langle B[\mathbf{\Gamma}(t;\varphi(t)=\varphi_P)]\rangle &= \langle B[\mathbf{\Gamma}(0;\varphi(0)=\varphi_P)]\rangle-\beta\int_0^t ds F_e(\varphi_P-\omega s) \\ &\quad\times\langle B[\mathbf{\Gamma}(s;\varphi(s)=\varphi_P)]J[\mathbf{\Gamma}(0;\varphi(0)=\varphi_P-\omega s)]\rangle. \qquad (15)\end{aligned}$$

That this equation is the time integral of Eq. (14) is most easily seen by noting that at $t=0$ it is an identity, and that differentiation of Eq. (15) yields Eq. (14).

The average value $\langle B(\mathbf{\Gamma}(t);\varphi(t)=\varphi_P)\rangle$ in Eq. (15) means the average over all values of phase $\mathbf{\Gamma}$, at time t, for a particular chosen constant value φ_P of the phase angle at time t, $\varphi(t)$; $\varphi(t)=\varphi_P$. If all possible values of φ_P from the interval $[0,\omega T_e]$ are substituted into Eq. (15), the dependence of $\langle B(\mathbf{\Gamma}(t);\varphi(t)=\varphi_P)\rangle$ on φ_P at the time t can be found. It should be pointed out that this dependence cannot be obtained by direct calculations from a set of trajectories starting from the *single* initial value of $\varphi(0)$, as shown in Fig. 3. Such a set could only give the value of $\langle B(\mathbf{\Gamma}(t);\varphi(t)=\varphi_0+\omega t)\rangle$ at the time t, $\langle B(\mathbf{\Gamma}(t+\delta t);\varphi(t)=\varphi_0+\omega(t+\delta t))\rangle$ at the time $t+\delta t$, etc. It should also be observed that in the integrals on both sides of Eq. (15), φ is a constant equal to φ_P. However, as the time s changes, phase-space trajectories which contribute to the correlation function at some particular value of s change. For different times s they start at different initial values of $\varphi_0=\varphi_P-\omega s$. Therefore, in order to find the evolution of $\langle B(\mathbf{\Gamma}(t);\varphi(t)=\varphi_P)\rangle$ for the chosen value of $\varphi(t)=\varphi_P$, we need to know the behavior of trajectories with *all* possible initial $\varphi(0)$ at all previous times.

Expression (15) is the general expression for the nonlinear response to a time-periodic external field. For time-independent fields, there is no φ dependence in the distribution function, and all extended phases that differ only in the extended phase-space coordinate φ become identical, so that Eq. (15) reduces to the TTCF formula for autonomous systems [3],

$$\langle B(\mathbf{\Gamma}(t))\rangle=\langle B(\mathbf{\Gamma}(0))\rangle-\beta F_e\int_0^t ds\langle B(\mathbf{\Gamma}(s))J(\mathbf{\Gamma}(0))\rangle. \qquad (16)$$

The linear time-dependent response formula [1], applicable in the low-amplitude or high-frequency limit, is obtained from Eq. (15) if the equilibrium correlation function is substituted for the transient correlation in the integrand of Eq. (15), keeping in mind that in equilibrium there is no φ dependence in $B(t)$ or $J(t)$. After substituting $s'=t-s$, we obtain

$$\begin{aligned}\langle B(\mathbf{\Gamma}(t))\rangle &= \langle B(\mathbf{\Gamma}(0))\rangle-\beta\int_0^t ds' F_e(s') \\ &\quad\times\langle B(\mathbf{\Gamma}(t-s'))J(\mathbf{\Gamma}(0))\rangle. \qquad (17)\end{aligned}$$

The general formula (17) has been derived for systems thermostated using the Gaussian thermostat (2). However, analogous formulas can be derived for adiabatic and canonical systems, systems thermostated with different thermostats or with other types of constraints, for example microcanonical, isobaric, or isoenthalpic.

III. TEST SYSTEM: COLOR CONDUCTIVITY

The formalism described in the Sec. II is illustrated by the example of nonequilibrium molecular dynamics simulation of a system of two disks with periodic boundary conditions, subject to the time-dependent color field [8]. The equations of motion are

$$\dot{\mathbf{q}}_i=\frac{\mathbf{p}_i}{m},$$
$$\dot{\mathbf{p}}_i=\mathbf{F}_i+\mathbf{i}c_iF_c(t)-\alpha\mathbf{p}_i, \quad i=1 \text{ and } 2. \tag{18}$$

The interaction $\mathbf{F}_i$ between disks is characterized by the WCA (Weeks-Chandler-Anderson) pair potential [9],

$$U(r)=\begin{cases} 4\varepsilon\left[\left(\frac{\sigma}{r}\right)^{12}-\left(\frac{\sigma}{r}\right)^{6}\right]+\varepsilon & \text{for } r<2^{1/6}\sigma \\ 0 \quad \text{for } r>2^{1/6}\sigma, \end{cases}$$

where σ is the effective diameter of the disks, ϵ the depth of the potential well of the corresponding Lennard-Jones potential, and $r=|\mathbf{q}_1-\mathbf{q}_2|$ is the distance between disks 1 and 2.

The disks differ by color labels, $c_i=(-1)^i$, $i=1$ and 2, which determine the interaction of each disk with the external color field $F_c(t)$ acting in the x direction. We assume a sinusoidal time dependence,

$$F_c(t)=\Theta(t)F_0\sin(\varphi_0+\omega t),$$

where the Heaviside function $\Theta(t)$ denotes the fact that the field starts to act upon the system at $t=0$.

The system is thermostated using the Gaussian thermostat. It should be mentioned here that in an N-body system the temperature is defined from the peculiar particle velocities relative to the streaming velocity of each species. However, in the special case of just two particles, there are not enough degrees of freedom to define both the streaming velocity and the peculiar velocities. Therefore we define a *temperaturelike* variable T using the laboratory kinetic energy,

$$k_BT/2=\sum_{i=1,2}\mathbf{p}_i^2/2m\equiv K, \tag{19}$$

where k_B is the Boltzmann constant. The temperaturelike variable T, as well as the total kinetic energy, are constrained to constant values using the Gaussian multiplier α,

$$\alpha=\frac{\sum_{i=1,2}(\mathbf{F}_i+\mathbf{i}c_iF_c)\cdot\mathbf{p}_i}{\sum_{i=1,2}\mathbf{p}_i^2}. \tag{20}$$

For this system, the phase space is defined as $\mathbf{\Gamma}=(\mathbf{q}_i,\mathbf{p}_i)$, $i=1$ and 2. The additional coordinate φ can be defined as

$$\varphi(t)=\varphi+\omega t, \tag{21}$$

so that the equations of motion for $t>0$ in *extended* phase space $\mathbf{\Gamma}'=(\mathbf{q}_i,\mathbf{p}_i,\varphi)$, $i=1$ and 2, are

$$\dot{\mathbf{q}}_i=\frac{\mathbf{p}_i}{m},$$
$$\dot{\mathbf{p}}_i=\mathbf{F}_i+\mathbf{i}c_iF_0\sin\varphi-\alpha\mathbf{p}_i, \tag{22}$$
$$\dot{\varphi}=\omega,$$

with the thermostating term α given by Eq. (20), and $\mathbf{q}_i\equiv(x_i,y_i)$, etc.

In this system, the equilibrium distribution function $f_0'(\Gamma')$ Eq. (7), is independent of φ, and $(\partial/\partial\mathbf{\Gamma}')\cdot[\dot{\mathbf{\Gamma}}'f_0'(\mathbf{\Gamma}')]$ in Eq. (12) is given by

$$\frac{\partial}{\partial\mathbf{\Gamma}'}\cdot[\mathbf{\Gamma}'f_0'(\mathbf{\Gamma}')]=-\beta F_c(\varphi_0)f_0'(\mathbf{\Gamma}')VJ_x(\mathbf{\Gamma}'), \tag{23}$$

where

$$J_x=\frac{1}{V}\sum_{i=1,2}c_i\dot{x}_i \tag{24}$$

is the color current density. It should be observed that for the two-particle system thermostated using Eqs. (18), (19), and (20), the magnitude of the color current cannot increase beyond a saturation value which can be determined from its constant kinetic energy (19). An external field of even increasing magnitude would cause an increase in the magnitudes of the x components of particle velocities. In the limit of $F_e\to\infty$, $K=(p_{1x}^2+p_{2x}^2)/2m$ can increase only to the maximum value determined from condition (19),

$$\max\{(p_{1x}^2+p_{2x}^2)/2m\}=\max\{p_{1x}^2/m\}=k_BT/2,$$

i.e.,

$$\max\{|p_{1x}|\}=(mk_BT/2)^{1/2} \quad \text{and} \quad \max\{|\dot{x}_1|\}=(k_BT/2m)^{1/2}.$$

Since $J_x=(\dot{x}_1-\dot{x}_2)/V=-2\dot{x}_1/V=-n\dot{x}_1$, where n is the number density $n=2/V$, the saturation color current is

$$\max\{|J_x|\}=n(k_BT/2m)^{1/2}. \tag{25}$$

We also define a microscopic pressurelike variable of this two-particle two-dimensional system,

$$P=\frac{1}{2}(P_{xx}+P_{yy})=\frac{1}{2V}\left\langle\sum_{i=1}^{N}\left(\frac{p_{xi}^2+p_{yi}^2}{m}+x_iF_{xi}+y_iF_{yi}\right)\right\rangle. \tag{26}$$

In this expression, the term corresponding to the kinetic part of the pressure consists of the contribution of the total rather than peculiar momenta, since the peculiar velocity has no meaning in the two-particle system. Because of the thermostating (18), (19), and (20), the total kinetic energy is fixed, and the ''kinetic part'' of P is a constant equal to k_BT. The other two terms in the sum are exactly equal to the configurational part of the pressure.

We monitored the response of $J_x'=(V/N)J_x$, which is proportional to the color current density (24), and the pressure-like variable P, Eq. (26), to sinusoidal color field as a function of the angle φ and time t. Since the color current is a linear function of momenta, the current response has a

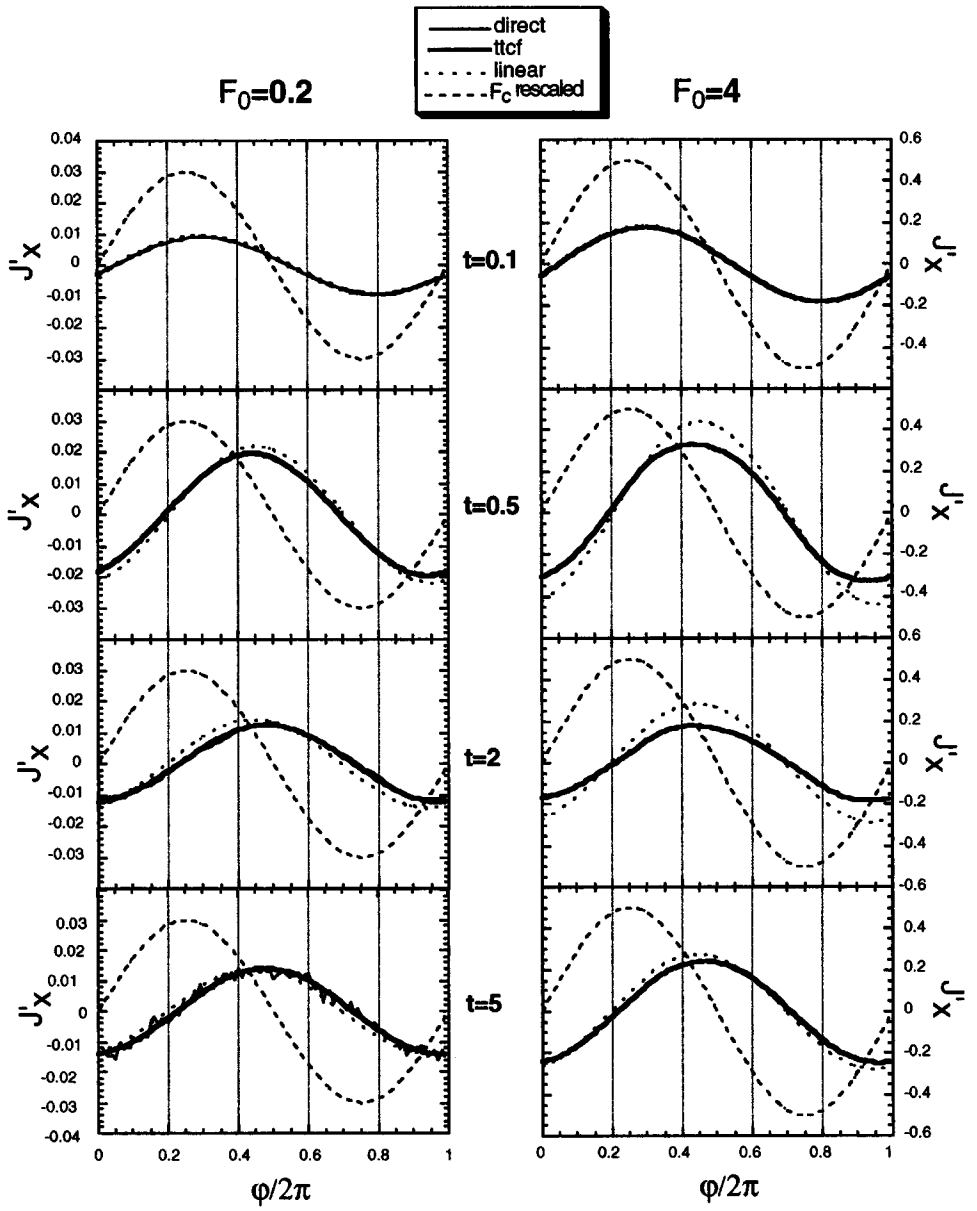

FIG. 4. Color current $J_x'=(1/N)\Sigma c_i\dot{x}_i$ as a function of the angle φ at different times after the color field has been applied. The results of the direct simulation, time-dependent TTCF, and linear approximation are compared for two amplitudes of the color field. For the lower amplitude $F_0=0.2$ all three methods give similar results, and for the higher amplitude $F_0=4$ the amplitude of the linear approximation response is higher than the other two, which cannot be distinguished in the graphs. The dashed line represents the rescaled external field, to show the development of the phase lag. The maximum allowed value for J_x' is $(k_BT/2m)^{1/2}$, and for this particular computer experiment it is $(0.5)^{1/2}=0.707\,107$.

strong linear component for weaker fields and the results of the time-dependent TTCF simulation could be compared to the results of the linear-response theory. The equilibrium correlation function $\langle P(t)J_x(0)\rangle$ under the time integral in Eq. (17) vanishes at all times, and there is no linear response for the pressure. The observed response in the pressure is therefore a strictly nonlinear effect, and provides a powerful test of our theory.

IV. RESULTS: COLOR CURRENT

The response of the color current density to sinusoidal color field has been monitored as a function of the angle φ and time t, and, since in equilibrium $\langle J_x(\mathbf{\Gamma}(0);\varphi)\rangle=0(\forall\varphi)$, Eq. (15) reduces to

$$\langle J_x(\mathbf{\Gamma}(t);\varphi(t)=\varphi_P)\rangle = -\beta V\int_0^t ds\; F_c(\varphi_P-\omega s)\langle J_x(\mathbf{\Gamma}(s);\varphi(s)=\varphi_P) \times J_x(\mathbf{\Gamma}(0);\varphi(0)=\varphi_P-\omega s)\rangle. \quad (27)$$

The simulations were done at the reduced density $\rho^*=\rho\sigma^2=0.396\,850$ and at the reduced temperature $T^*=k_BT/\epsilon=1.0$, using the fourth-order Runge-Kutta method of integration of the equations of motion (20) with a time step of $\delta t=0.002$. The interval $[0,2\pi]$ of possible values of the angle φ has been divided into 100 subintervals, and the time step of time integration in Eq. (27) is therefore

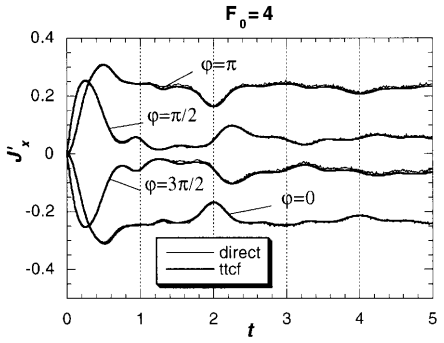

FIG. 5. The time evolution of the color current J_x' at four angles φ for the color field amplitude $F_0=4$.

$ds=0.01$. From each starting phase $\mathbf{\Gamma}=(\mathbf{q}_i,\mathbf{p}_i)$ of the isokinetic equilibrium ensemble, an additional starting point was generated using the time-reversal mapping $\mathbf{M}^T(\mathbf{\Gamma})=(\mathbf{q}_i, -\mathbf{p}_i)$, in order to improve the statistics and to reduce the systematic error. This additional starting phase point ensures that the average initial current is identically zero.

The color current response has been monitored for a range of color field amplitudes at the frequency of $\omega/2\pi$ equal to unity. Figure 4 shows the evolution of the color current response for two amplitudes of the color field, $F_0=0.2$ and 4, as a function of the angle $\varphi(t)$ at different times, from direct simulation and using the transient time correlation function approach. Since the objective of this simulation has been to test whether the direct calculations and our theory (27) coincide, we used a large number of initial trajectories, $2\times60\,000$ for each of the 100 values of $\varphi(0)$ for the weaker field, and $2\times18\,000$ for the stronger field where the results of direct simulations were less noisy.

In Fig. 4, shortly after the color field started to act upon the system, at $t=0.1$, the response is of very low amplitude and almost in phase with the field. In time, the phase lag and the amplitude change until they reach the value of the final state. The corresponding linear response was evaluated using the time-dependent response formula (17) and compared to the direct simulation and TTCF results. The equilibrium correlation function in Eq. (17) has been calculated from 3×10^7 trajectories using the shift register technique [10]. In our calculations the shift register was not filled at every time step, but there was a waiting period of 500 time steps between the starting points of old and new trajectories.

In the case of the lower amplitude in Fig. 4 the direct and TTCF methods agree within the experimental error, although there is still some noise in the direct results at $t>2$, and the amplitude of the linear response is only slightly larger. However, for the higher amplitude of the color field in Fig. 4, the amplitude of the linear approximation is about 8% higher in the final state than the one obtained by direct simulation, whereas the direct simulation and TTCF results agree to within 1% and cannot be distinguished in the graph.

The time evolution of the color current response for five periods of color field F_c of the amplitude $F_0=4$ for four different angles φ, obtained from the same simulation as above, is shown in Fig. 5. The correspondence of the direct simulation and the TTCF results is remarkable at all times.

In Fig. 6, the trajectories starting at the same initial angle $\varphi_0=0$ are followed over five periods of the color field. Again, the linear approximation results agree reasonably well with the direct simulation and TTCF results in the case of the lower amplitude of the color field $F_0=0.2$, but for the higher-field amplitude $F_0=4$ the oscillations predicted by the linear approximation are larger than the direct simulation and TTCF results. It is obvious that the linear approximation should fail at larger fields, since it predicts that the amplitude of J_x' increases linearly with the amplitude of the field, and thus can exceed the maximum allowed amplitude $\max\{|J_x'|\}=(k_BT/2m)^{1/2}=0.707$, which is an impossible result. However, even at a field of the amplitude $F_0=4$ the induced current is only 35% of its saturated value, and we should not be too surprised that the linear theory is a reasonable approximation. The response obtained by the TTCF method coincides with the direct simulation for $F_0=4$.

The main advantage of the time-dependent TTCF method lies in its efficiency in noise reduction, especially for fields of low amplitude. In Fig. 7 the results of the direct simulation and TTCF at $t=5$ obtained from the simulations from 2×5000 and $2\times60\,000$ for each φ are compared for $F_0=0.2$ and from 2×5000 and $2\times18\,000$ for $F_0=4$. For the lower-field amplitude there is considerable noise reduction in the direct simulation results with the increased number of trajectories, but the result is still quite noisy. The TTCF results, on the other hand, are smooth and hardly change at all, which means that the correct statistics can be obtained with less trajectories by using the TTCF method. Figure 7 also shows that the direct simulation is much more efficient for high-field amplitudes ($F_0=4$) than for low amplitudes, although the TTCF results are still smoother than the direct results.

In order to compare the efficiency of the two methods for calculating the color current response at a range of field amplitudes, we performed two sets of simulations using $2\times10\,000$ trajectories for each value of φ, and used the discrepancy in the results to estimate the error of simulation $\Delta J_x'/F_0$. The mean error was calculated as the mean value of half the discrepancy of the responses for the external fields starting at $\varphi_0=0$ over the time interval $\Delta t=5$, and the maximum error is the maximum of half the discrepancy over the same period. Figure 8 shows that for the fields of the amplitude of less than about $F_0=2.5$ the mean error of the direct method is larger than the mean error of the TTCF method, and TTCF is clearly more efficient. For $F_0\geqslant2.5$ the mean errors and hence the efficiencies of both methods become comparable. The maximum errors Fig. 8 are, however, consistently lower for the TTCF method, because the latter yields averages which are smoother.

The Green-Kubo linear-response theory can be used to estimate the expected error in direct calculations of color current. In the low-field limit the standard deviation in the current density J' is independent of the external field [11], and therefore $\Delta J_x'/F_0x$ should be inversely proportional to the field amplitude. The $y\propto F_0^{-1}x$ fits to the mean and maximum errors of direct calculations, shown in Fig. 8 as dashed lines, show that this proportionality is roughly satisfied. The errors in the TTCF calculations seem to be field independent, but are always smaller than those for the direct calculations.

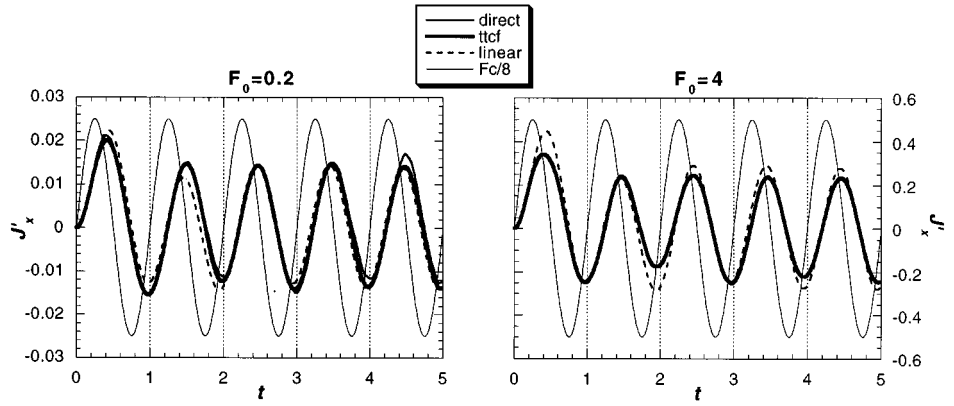

FIG. 6. The time evolution of the color current J_x' from the trajectories which all start from the same initial angle $\varphi_0=0$. For a lower-field amplitude $F_0=0.2$, the color currents, evaluated by direct calculation, using the time-dependent TTCF method and the linear approximation, are comparable. For the higher-field amplitude $F_0=4$ the linear response theory gives oscillations that are too large, and the results of the direct and TTCF methods coincide on the diagram. The thin line is the rescaled external field.

V. RESULTS: HYDROSTATIC PRESSURE

The TTCF expression for the ''hydrostatic pressure'' derived from Eq. (15) is

$$\langle P(\mathbf{\Gamma}(t);\varphi(t)=\varphi_P)\rangle=\langle P(0)\rangle-\beta V\int_0^t ds\ F_c(\varphi_P-\omega s)\times\langle P(\mathbf{\Gamma}(s);\varphi(s)=\varphi_P)\times J_x(\mathbf{\Gamma}(0);\varphi(0)=\varphi_P-\omega s)\rangle. \tag{28}$$

In Figures 9, 10, and 11 we show the results obtained by the direct simulation and the time-dependent TTCF method for 1.1×10^5 trajectories for each of the 100 values of φ for the field amplitude of $F_0=3$. The pressure oscillates with twice the frequency of the external field (since it is an even function of momenta and therefore depends only on the magnitude and not on the sign of the external field). Since the effect is very small, the direct simulation data are very noisy, and therefore there is still some disagreement at early times. At late times, the agreement between the two sets of calculations is excellent. This agreement is all the more remarkable because of the complex shape of the response curves and the fact that these responses are entirely nonlinear. The chance of accidental agreement, particularly in Fig. 10, must be negligible.

In Fig. 10 we see the response for $\varphi(t)=0,\pi$, and for $\varphi(t)=\pi/2,3\pi/2$. By symmetry the response in each of these pairs should be identical. The disparity in this gives a reasonable estimate of the statistical uncertainty in the TTCF and the direct response curves.

Figure 11 shows the pressure responses obtained from direct simulations and TTCF results for fields of the ampli-

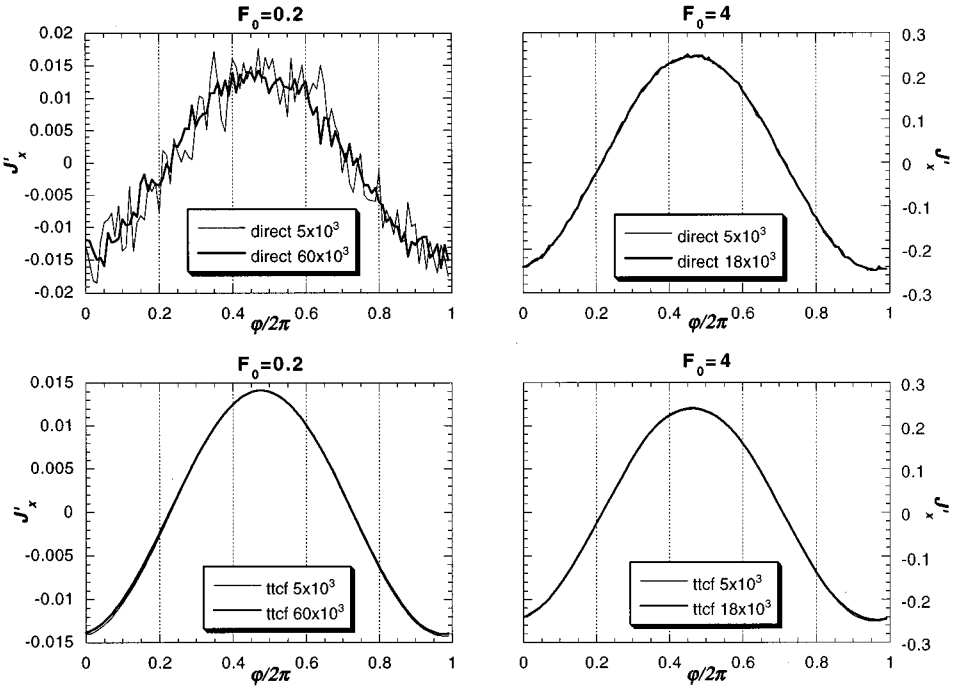

FIG. 7. Illustration of the efficiency of the time dependent TTCF method in noise elimination. For the lower field amplitude $F_0=0.2$, the noise is somewhat reduced in the results from $2\times60\,000$ trajectories for each φ compared to the results from 2×5000 trajectories. TTCF results, however, do not differ much, suggesting that good statistics can be obtained from less trajectories. For the higher amplitude $F_0=4$, the direct method is much more efficient than for the lower field, but the TTCF results are still smoother.

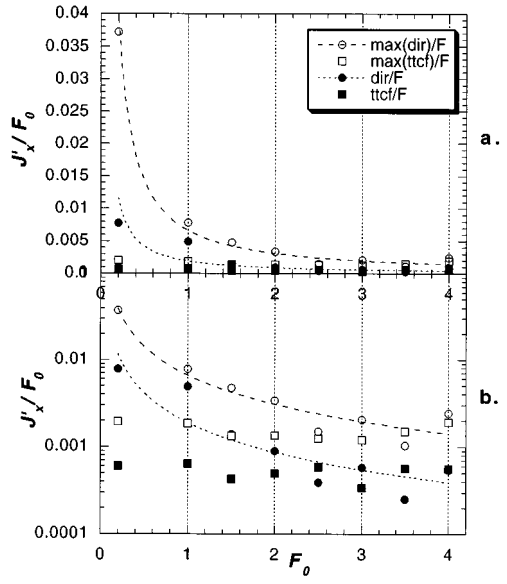

FIG. 8. (a) Simulation errors of the color current response for a range of field amplitudes from two sets of simulations of $2\times10\,000$ trajectories for each field. The mean error is the average error from two responses to the field starting with $\varphi(0)=0$ over a time interval of $\Delta t=5$, the maximum error is the largest error in this interval. The assumption of $1/F_0$ dependence of the direct simulation errors on the field amplitude gives a reasonably good fit. (b) Mean errors become comparable for $F_0\geqslant 2.5$, but the maximum error is always larger for the direct simulations, which is better seen in the logarithmic plot.

tude $F_0=3$ starting at $\varphi_0=0$ and $\varphi_0=\pi/2$. The dotted lines represent the rescaled external field. The response for $\varphi_0=\pi$ should be equal to the response for $\varphi_0=0$ because the field differs only in sign, and the response for $\varphi_0=\pi/2$ should equal the response for $\varphi_0=3\pi/2$. The disparity between the responses at $\varphi_0=0$ and $\varphi_0=\pi$ was used to estimate the simulation error $\Delta(\Delta P)/F_0$ depending on the field amplitude. We used $2\times10\,000$ trajectories for each φ at each field amplitude to obtain the responses, and plotted the average discrepancies over the time interval of $\Delta t=5$ against the field amplitude in Fig. 12. Although the direct and time-dependent TTCF curves are computed from the same number of simulation time steps, the TTCF curves always have a smaller variance. This is somewhat surprising given that the field amplitude is so large, since the TTCF methods will always be more efficient than direct methods at sufficiently small fields. We believe that this improvement in efficiency is related to the fact that, in Eq. (15), the response at a given time and specified phase angle is computed from an ensemble average of trajectory responses which span the initial phase angle distribution. This cross-phase-averaging results in superior efficiency.

VI. CONCLUSION

The generalization of the TTCF formalism to nonautonomous systems was developed by extending the phase space

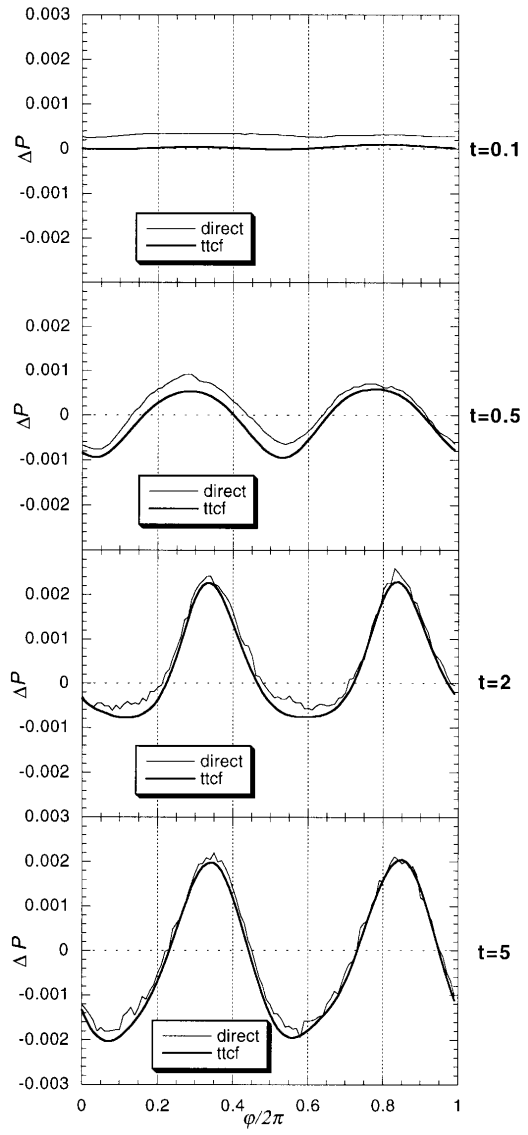

FIG. 9. The direct simulation and TTCF results for the pressure as a function of φ at different times after the color field of $F_0=3$ has been applied. The pressure oscillates with twice the frequency of the field.

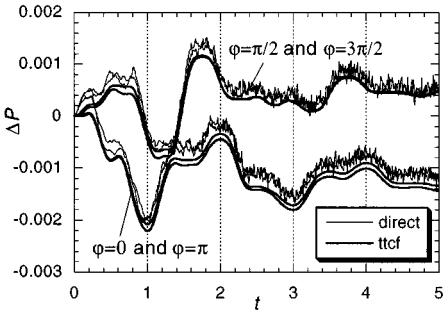

FIG. 10. The time dependence of the pressure at four angles φ for the color field amplitude $F_0=3$. The responses at $\varphi(0)=0$ and $\varphi(0)=\pi$ should be equal by symmetry, as well as the responses at $\varphi(0)=\pi/2$ and $\varphi(0)=3\pi/2$, which can give an estimate of the error of simulation.

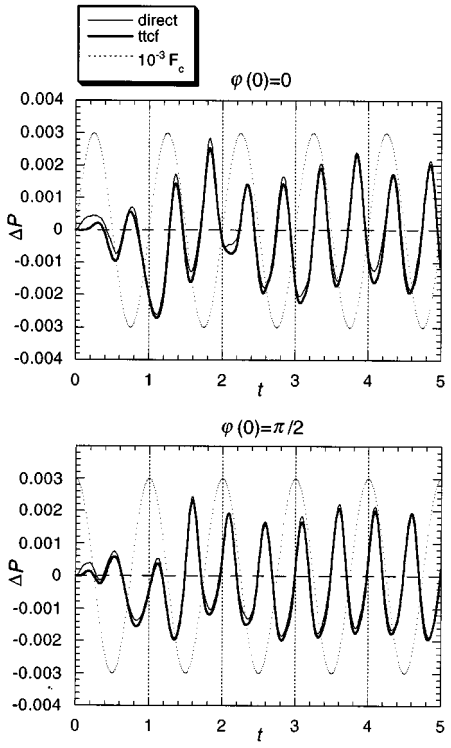

FIG. 11. The responses to the external fields starting at $\varphi(0)=0$ and $\varphi(0)=\pi/2$ for $F_0=3$. The response at $\varphi(0)=\pi$ should equal the response at $\varphi(0)=0$, and for $\varphi(0)=3\pi/2$ should equal $\varphi(0)=\pi/2$ because the corresponding fields differ only in sign.

to include an additional coordinate φ, which is linearly dependent on time and which is incorporated into the equations of motion. The *linear* time dependence of this additional phase-space coordinate is essential for the development of the extended TTCF algorithm, because it enables one to reach exactly the prescribed values of φ after a given number of time steps. The equations of motion in the *extended* phase space become autonomous, and the response is governed by the time evolution of the probability distribution $f'(\mathbf{\Gamma}')$ of the extended phase space as a whole. Therefore, in order to calculate the response, it is necessary to use initial equilibrium phases $\mathbf{\Gamma}'(0)$ distributed over all possible values of φ, as well as over all possible values $(\mathbf{q},\mathbf{p})$. In the direct method, one observes a set of initial phases on a hyperplane $\varphi(0)=\varphi_P-\omega t$, as it evolves in time while the phase-space distribution relaxes from equilibrium $f_0(\mathbf{\Gamma}')$ to the steady-state $f_\infty(\mathbf{\Gamma}')$ form. The extended TTCF method, however,

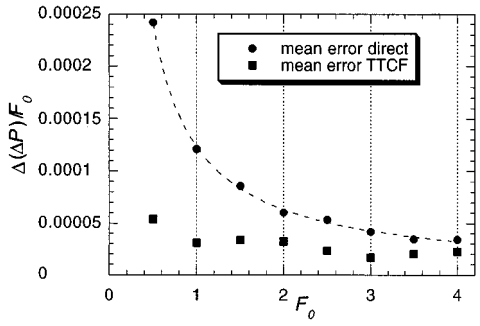

FIG. 12. Dependence of the simulation error on the field amplitude. The error of simulation calculated from $2\times10\,000$ trajectories per φ for each field amplitude is found from the average discrepancy between the responses for $\varphi(0)=0$ and $\varphi(0)=\pi$ over the time interval of $\Delta t=5$. Again, the $1/F_0$ dependence of the direct simulation errors on the field amplitude gives a good fit.

looks only at one hyperplane $\varphi=\varphi_P$ all the time, and uses only the phases on this hyperplane, as they arrive from different initial coordinates $\varphi(0)$, to evaluate the average as $f(\mathbf{\Gamma}',t)$ changes in time. It is therefore not surprising that trajectories starting at all possible extended phase-space coordinates φ play a role in calculations of $\langle B[\mathbf{\Gamma}(t;\varphi(t)=\varphi_P)]\rangle$, i.e., the average of B over a particular hyperplane $\varphi=\varphi_P$ of $\mathbf{\Gamma}'$ at the time t when the average is evaluated using the time-dependent TTCF algorithm.

The simulation results for the test case of the response of the color current to a sinusoidal color field for a periodic two-disk system, shows excellent agreement between the extended TTCF approach and the direct simulation. The comparison of results for the intrinsically nonlinear field induced pressure shift is even more impressive. Even at comparatively large fields, the extended TTCF approach yields results with superior computational efficiency to direct simulation. This enhanced efficiency is thought to result from the nondeterministic sampling of the phase angle. This sampling results in an efficient exploration of the extended phase space.

One disadvantage of this theory is that it can only be applied to periodic fields. Another disadvantage is that the results are relevant only to periodic fields of the same frequency and wave form. For example, we cannot use the results of the present simulations for sinusoidal fields to predict the response of the same system to strong square-wave fields, or indeed, to sinusoidal fields of different frequencies.

[1] M. S. Green, J. Chem. Phys. **22**, 398 (1954); R. Kubo, J. Phys. Soc. Jpn. **12**, 570 (1957).

[2] R. Zwanzig, Annu. Rev. Phys. Chem. **16**, 67 (1965); R. Zwanzig, *Lectures on Theoretical Physics* (Wiley Interscience, New York, 1961), Vol. III, p. 135.

[3] W. M. Vischer, Phys. Rev. A **10**, 2461 (1974); J. W. Dufty and M. J. Lindenfeld, J. Stat. Phys. **20**, 259 (1979); E. G. D. Cohen, Physica A **118A**, 17 (1983); G. P. Morriss and D. J. Evans, Mol. Phys. **54**, 629 (1985); Phys. Rev. A **35**, 792 (1987).

[4] T. Yamada and K. Kawasaki, Prog. Theor. Phys. **38**, 1031 (1967).

[5] J. Petravic and D. J. Evans, Phys. Rev. Lett. **78**, 1199 (1997).

[6] D. J. Evans and G. P. Morriss, Mol. Phys. **64**, 521 (1988); B. L. Holian and D. J. Evans, J. Chem. Phys. **83**, 3560 (1985).

[7] D. J. Evans and G. P. Morriss, *Statistical Mechanics of Non-*

equilibrium Liquids (Academic, New York, 1990).
[8] D. J. Evans, W. G. Hoover, B. H. Failor, B. Moran, and A. J. C. Ladd, Phys. Rev. A **28**, 1016 (1983).
[9] J. D. Weeks, D. Chandler, and H. C. Andersen, J. Chem. Phys. **54**, 5237 (1971).
[10] M. P. Allen and D. J. Tildesley, *Computer Simulation of Liquids* (Clarendon, Oxford, 1987).
[11] D. J. Evans and D. J. Searles, Phys. Rev. E **52**, 5839 (1995).